

# Numerical Simulation of Heavy Particle Dispersion Time Step and Nonlinear Drag Considerations

Lian-Ping Wang<sup>1</sup>

D. E. Stock

Department of Mechanical  
and Materials Engineering,  
Washington State University,  
Pullman, WA 99164-2920

*Numerical experiments can be used to study heavy particle dispersion by tracking particles through a numerically generated instantaneous turbulent flow field. In this manner, data can be generated to supplement physical experiments. To perform the numerical experiments efficiently and accurately, the time step used when tracking the particles through the fluid must be chosen correctly. After finding a suitable time step for one particular simulation, the time step must be reduced as the total integration time increases and as the free-fall velocity of the particle increases. Based on the numerical calculations, we suggest that the nonlinear drag be included in a numerical simulation if the ratio of the particle's Stokes free-fall velocity to the fluid rms velocity is greater than two.*

## Introduction

Numerical experiments enable us to advance our understanding of particle motion in a turbulent flow. While physical experiments are vital, they are difficult to carry out and often do not provide all the information we seek. For example, particle motion is easiest to express and simulate in terms of Lagrangian statistics, but this information is very difficult to obtain experimentally. Numerical experiments must be performed carefully to ensure that the resulting data represent reality, and they must also be done efficiently to allow numerous parameters to be examined. The purpose of the work described here was to provide some guidelines to help researchers doing numerical experiments for gas-particle flows decide what time step to use and when Stokes drag can no longer be used.

Numerical experiments for gas-particle flows involve tracking the particles through a simulated turbulent flow. The instantaneous turbulent field can be found by solving the Navier-Stokes equations. This can be done by direct numerical simulation (e.g., Squires and Eaton 1989; Ueda et al. 1983). Unfortunately, direct simulations are still limited to very low Reynolds numbers and are often prohibitively time consuming. There are many alternative techniques (e.g., Monte-Carlo procedure, random flight model, Brown-Hutchinson (1979) model) to generate instantaneous turbulent flow and then simulate particle dispersion. These alternative techniques are stochastic models and can give reasonable agreement with experimental data, but they require that certain assumptions be made about the fluid-particle interaction and use empirical coefficients such as a diffusion coefficient or Lagrangian time and length scales.

In this paper, we apply the model proposed by Kraichnan (1970) in which a stationary Gaussian velocity field is generated by means of a linear superposition of a large number of random

Fourier modes. This model falls between the very complicated techniques of direct simulation and the simplified approach of the more common stochastic techniques. Unlike direct simulations, there is no limitation on Reynolds number for this model. All the parameters involved are Eulerian and the spectrum and autocorrelation of the flow can be specified. Kraichnan's model is very efficient for this particular simulation because it computes the velocity at the time and location required, and interpolation is not required as it is with direct simulation. While Kraichnan's model is limited to isotropic and homogeneous turbulence, which is an idealized situation, many regions of a flow field are closely represented by this flow.

Particle velocities and trajectories are found by numerically integrating the Lagrangian equations describing the particle motion with inertia and external body forces included in the equations of motion for the particle. All the statistics of the particle's motion are evaluated by ensemble averaging over a large number of realizations of individual particles.

## Simulation of the Turbulent Flow Field

The stochastic model for the Gaussian random velocity field proposed by Kraichnan (1970) has been widely used to simulate stationary homogeneous turbulence (e.g., Maxey 1987; Reeks 1980). Recently this model has been extended by Drummond et al. (1984) and others to incorporate more turbulent characteristics into the model. For the purpose of the present work, the original model is sufficient and requires less information about the flow being simulated. In Kraichnan's method, the flow field is represented by the following equation, which is a linear superposition of a large number of Fourier modes with random amplitudes and phases:

$$u_i(x_i, t)/u_0 = \sum_{n=1}^N \{ b_i^{(n)} \cos(\mathbf{k}^{(n)} \cdot \mathbf{x} + \omega^{(n)} t) + c_i^{(n)} \sin(\mathbf{k}^{(n)} \cdot \mathbf{x} + \omega^{(n)} t) \}. \quad (1)$$

<sup>1</sup>Current Address: Center for Fluid Mechanics, Turbulence, and Computation, Brown University, Providence R.I., 02912.

Contributed by the Fluids Engineering Division for publication in the JOURNAL OF FLUIDS ENGINEERING. Manuscript received by the Fluids Engineering Division September 21, 1989.

This equation is equivalent to the discretization of a Fourier transform of the velocity field over space and time. Here  $N$  is the number of modes and  $u_0$  is the rms fluctuation velocity. The mean velocity is zero, and the velocity field is understood to represent the velocity field in a frame of reference moving with the mean velocity of the flow. Using the definitions given in Wang and Stock (1988), Eq. (1) gives the velocity field in the moving Eulerian system. For each  $n$ ,  $k_i^{(n)}$  and  $\omega^{(n)}$  are chosen independently from Gaussian random numbers of zero mean with standard deviations of  $k_0$  and  $\omega_0$ , respectively. Real coefficients  $b_i^{(n)}$  and  $c_i^{(n)}$  are also independent Gaussian random variables that have been filtered such that  $b^{(n)} \cdot \mathbf{k}^{(n)}$  and  $c^{(n)} \cdot \mathbf{k}^{(n)}$  vanish, making the overall flow field incompressible. The ensemble-averaged two-point correlation of this random flow field is (Maxey, 1987)

$$R_{ij}(\mathbf{r}, \tau)/u_0^2 = N \int_{-\infty}^{\infty} d^3\mathbf{k} \int_{-\infty}^{\infty} d\omega \times P_1(\mathbf{k})P_2(\omega)\Gamma^2(\mathbf{k}, \omega) \left[ \delta_{ij} - \frac{k_i k_j}{k^2} \right] \cos(\mathbf{k} \cdot \mathbf{r} + \omega\tau) \quad (2)$$

where  $P_1$  and  $P_2$  are Gaussian probability functions and  $\Gamma(k, \omega)$  is the scaling function.  $\Gamma(k, \omega)$  allows the flow field to be generated with any prescribed two-point correlation function. If

$$\text{we assume } \Gamma \text{ is only a function of } k = \sqrt{k_1^2 + k_2^2 + k_3^2}, \text{ then}$$

$$R_{ij}(\mathbf{r}, \tau)/u_0^2 = \frac{N}{(2\pi)^{3/2}k_0^3} \int_{-\infty}^{\infty} d^3\mathbf{k} \Gamma^2(k) \left[ \delta_{ij} - \frac{k_i k_j}{k^2} \right] \cos(\mathbf{k} \cdot \mathbf{r}) e^{-\frac{k^2}{2k_0^2} \exp\left(-\frac{\omega_0^2 \tau^2}{2}\right)} \quad (3)$$

The scalar energy-spectrum function associated with this flow field is

$$E(k) = \sqrt{\frac{2}{\pi}} \frac{k^2}{k_0^3} \Gamma^2(k) \exp\left(-\frac{k^2}{2k_0^2}\right) \quad (4)$$

In this work, the scaling function  $\Gamma$  was chosen to be

$$\Gamma(k, \omega) = \frac{k}{\sqrt{2Nk_0}} \quad (5)$$

which makes the energy spectrum function

$$E(k) = \frac{u_0^2}{\sqrt{2\pi}} \frac{k^4}{k_0^5} \exp\left(-\frac{k^2}{2k_0^2}\right) \quad (6)$$

This form of the energy spectrum has also been used by Kraichnan (1970) and Maxey (1987). The function in Eq. (6) has a maximum at  $k = 2k_0$ . The Eulerian one-point time correlation in the moving coordinate system is

$$D(\tau) = \exp\left(-\frac{\omega_0^2 \tau^2}{2}\right) \quad (7)$$

and Eulerian integral time scale in the moving coordinate system is

$$T_{mE} = \frac{\sqrt{2\pi}}{2\omega_0} \quad (8)$$

The flow field generated by this method is governed by three parameters,  $u_0$ ,  $k_0$ , and  $\omega_0$ , where  $u_0$  is the rms fluctuation velocity,  $k_0$  is the characteristic wave number which depends on the integral length scale of the turbulence, and  $\omega_0$  is related to the one-point integral time scale. Wang and Stock (1988) discussed how these three parameters can be related to the flow field found in grid generated turbulence.

### Simulation of Heavy Particle Motion

The general Lagrangian equations for particle motion in an unsteady flow are known as the BBO (Bassett-Boussinesq-Oseen) equation (Maxey and Riley, 1983) in which Stokes drag, virtual mass, pressure gradient, Basset history term, and buoyancy effects are included. In the present study, we assume that the particles are much denser than the gas and that the particulate phase is dilute. The pressure gradient force, the virtual mass force, and the Basset force can be neglected because of the large difference between the density of the gas and the density of the particles. Therefore the equations of motion for a particle can be written as

$$\frac{dv_i}{dt} = \frac{(u_i(\mathbf{y}, t) - v_i)f}{\tau_a} - q\delta_{i3} \quad (9)$$

### Nomenclature

$b_i, c_i$ = random coefficients	St = Stokes number	$\gamma$ = $v_d/u_0$
$d_p$ = diameter of particle	$t$ = time	$\Gamma$ = the scaling function, Eq. (2)
$D(\tau)$ = one-point fluid velocity correlation in the moving Eulerian frame	$T_{mE}$ = integral time scale of Eulerian fluid correlation in the moving Eulerian frame	$\nu$ = fluid kinematic viscosity
$E(k)$ = scalar energy spectrum function	$T_L$ = Lagrangian integral time scale of particle	$\omega$ = frequency
$f$ = the ratio of drag coefficient to Stokes drag	$\mathbf{u}$ = flow velocity	$\omega_0$ = characteristic frequency
$q$ = external body force acting on particle	$u_0$ = fluid rms fluctuation velocity	$\rho$ = fluid density
$\mathbf{k}$ = wave number	$\mathbf{v}$ = particle velocity	$\rho_p$ = particle density
$k_0$ = characteristic wave number	$v_{i0}$ = $i$ th component of particle rms fluctuation velocity	$\tau$ = time delay
$m$ = $k_0 u_0 T_{mE}$	$v_d$ = Stokes drift velocity of particle = $\tau_a q$	$\tau_a$ = particle aerodynamic response time
$N$ = the number of Fourier modes	$\mathbf{x}$ = Eulerian coordinate	
$\mathbf{r}$ = space separation	$\mathbf{y}$ = particle's location	
$R_{ij}(\mathbf{r}, \tau)$ = fluid velocity correlation	$\delta_{ij}$ = Kronecker delta	
$Re_0 = d_p u_0 / \nu$	$\epsilon_{ij}^p$ = particle diffusivity tensor	
$Re_p$ = particle Reynolds number		
		<b>Superscripts</b>
		$(j)$ = $j^{\text{th}}$ mode
		* = dimensionless variables
		<b>Subscripts</b>
		1, 2 or $x, y$ = horizontal directions
		3 or $z$ = vertical direction
		$e$ = effective parameter
		$i$ = $i^{\text{th}}$ component

$$\frac{dy_i}{dt} = v_i, \quad (10)$$

where  $v_i$  is the particle velocity and  $q$  is the body force per unit mass.  $u_i(y, t)$  is the fluid velocity at the location of the particle,  $y(t)$ .  $\tau_a$  is the aerodynamic response time for the linear Stokes drag, namely,

$$\tau_a = \frac{\rho_p d_p^2}{18\mu}, \quad (11)$$

where  $d_p$  is the diameter of particle,  $\mu$  is the dynamic viscosity of the fluid, and  $\rho_p$  is the material density of the particle. The factor  $f$  is the ratio of the drag coefficient to Stokes drag which is well represented for Reynolds number up to 1000 by the empirical expression

$$f = 1 + 0.15 \text{Re}_p^{0.687}, \quad (12)$$

where  $\text{Re}_p$  is the particle Reynolds number based on the relative velocity between the particle and the fluid. Equations (9) and (10) can be put into dimensionless form to give

$$\frac{dv_i^*}{dt^*} = \frac{(u_i^*(y^*, t^*) - v_i^*)f}{\text{St}} - \frac{\gamma \delta_{i3}}{\text{St}}, \quad (13)$$

$$\frac{dy_i^*}{dt^*} = v_i^*, \quad (14)$$

where the dimensionless variables are defined as  $v_i^* = v_i/u_0$ ,  $u_i^* = u_i/u_0$ ,  $y_i^* = y_i/(u_0 T_{mE})$  and  $t^* = t/T_{mE}$ .  $\text{St}$  is the Stokes number defined as  $\tau_a/T_{mE}$ , the ratio of the particle's aerodynamic response time (based on Stokes drag) to a characteristic time scale of the flow. The Stokes number is a measure of the relative importance of inertia since  $\tau_a$  increases with particle mass. The parameter  $\gamma$  is defined as  $\tau_a q/u_0 = v_d/u_0$ . It is the ratio of the particle's Stokes velocity to the rms fluid fluctuating velocity.

The initial conditions for the equations of motion of the particles are

$$y_i^*(t^* = 0) = 0, \quad (15)$$

$$v_i^*(t^* = 0) = u_i^*(0, 0) - \gamma \delta_{i3}. \quad (16)$$

These conditions are probably not realistic for particles being emitted from a point source, but in this study the numerical computation of particle dispersion was started at some later time, e.g.,  $t^* = 2$  to allow the initial conditions to have sufficient time to decay. Thus any spurious effects of the initial conditions on the long-time dispersion of the particles were eliminated.

Particles trajectories are found by numerically integrating the equations of motion for the particles, Eqs. (13) and (14), using fluid velocities from Eq. (1). The Gaussian random numbers used in Eq. (1) are determined by the functional routine RNNOF of the IMSL STAT/LIBRARY which is available on the IBM 3090 of Washington State University's Computer Center. The routine generates a Gaussian distribution by an inverse CDF technique. At each point on a particle trajectory where the fluid velocity is required it is computed using

$$u_i^*(y^*, t^*) = \sum_{n=1}^N \{ b_i^{(n)} \cos(k^{(n)*} \cdot y^* + \omega^{(n)*} t^*) + c_i^{(n)} \sin(k^{(n)*} \cdot y^* + \omega^{(n)*} t^*) \}, \quad (17)$$

where  $k_i^{(n)*}$  and  $\omega^{(n)*}$  are nondimensional Gaussian random numbers with zero mean and with standard deviations of  $m \equiv k_0 T_{mE} u_0$  and 1.2533 (or  $\sqrt{\pi}/2$ ), respectively. Then Eqs. (13) and (14) are integrated by the fourth-order, stable predictor-corrector scheme known as the Hamming method. The values for the first four steps are computed using the fourth-order Runge-Kutta method three times. The numerical error in the

integration increased exponentially with time. Therefore, it is critical to use a time step  $\Delta t^*$  small enough to satisfy a global tolerance accuracy but as large as possible to save time.

### Integration Time Step Size Considerations

The time step considered here is that used to numerically integrate the Lagrangian motion of a heavy particle, given that the instantaneous flow is a continuous function of space and time. Intuitively we know that the size of the time step for a given numerical accuracy is governed by the character of the turbulence, most likely the integral time scale, the particle's inertia, and the particle's free fall velocity. We carried out some tests to determine the relative importance of these three parameters.

Figure 1 shows typical trajectories in a  $y-z$  plane for a single particle with different inertia parameters ( $\text{St} = 0.1, 0.4, 1.0, 5.0$ ) and  $\gamma$  equal to zero. As the  $\text{St}$  number increases, the particle tends not to respond to the acceleration of the surrounding fluid, but instead follows a trajectory quite different than that of the fluid. From this figure it is difficult to guess if smaller time steps are required for a particle that follows the flow or one that is very sluggish. Figure 2 shows typical trajectories in a  $y-z$  plane for a single particle with different nondimensional free fall velocities,  $\gamma$  ( $\gamma = 0.0, 0.4, 1.0, 2.0$ ), for a  $\text{St}$  of 0.2. For small  $\gamma$ , the particle shows no preferred direction, but as  $\gamma$  increases the particle drifts in the direction of the body force. Again it is difficult to guess which case will require the smallest time step to hold the overall error at a constant value.

To quantify the effect of  $\text{St}$  number and  $\gamma$  on the size of the time step required to maintain a given overall tolerance, simulations were run and the error in the particle's displacement and velocity were compiled. Figure 3 shows the result of one such simulation. The errors were calculated relative to an almost exact trajectory obtained by a nondimensional time step of  $\Delta t^* = 0.01$ . The flow field used in this simulation is typical of that found in low speed gas-particle flows.<sup>2</sup> The error in the particle location grows exponentially with time. No matter how small the time step the error in the particle's location will ultimately start to increase in a manner similar to that shown in Fig. 3, except that the smaller the time step, the longer it will take for the error to become significant.

If the long-time diffusivities are to be calculated, one would like to have very low error in the particle trajectories after several Lagrangian integral times. Simulations were made for a range of Stokes numbers and  $\gamma$  to find the time step that would give a one percent error in particle location after a total integration time of  $4T_L^*$ .<sup>3</sup> Table 1 lists the time step size,  $\Delta t^*$ , that will give an average error of one percent in the particle's location after a total integration time of  $4T_L^*$ . The results clearly show that a smaller time step is required with increasing Stokes number and  $\gamma$ . The decrease in the length of the time step with increasing Stokes number (particle mass) is mostly due to the increase in the Lagrangian integral time. The decrease in time step with increasing  $\gamma$  (free-fall velocity) is caused by the increase in distance traveled by the particle.

If one is interested in the behavior of particle trajectories at a given time after release (e.g., for particles in a combustion chamber), then the time-step size limit should be determined for a fixed total integration time. Table 2 shows the time-step

<sup>2</sup>The rms fluctuation velocity of the flow,  $u_0$ , was 20 cm/s and the integral time scale,  $T_{mE}$ , was 14.4 ms. The Reynolds number based on these scales ( $T_{mE} u_0^2/\nu$ ) was about 50. These values are typical for grid-generated flow of air (e.g., Wells and Stock, 1983).

<sup>3</sup> $T_L^* = T_L/T_{mE}$ .  $T_L$  is the Lagrangian integral time scale for the motion of heavy particles. It is a strong function of  $\text{St}$  and a weak function of  $\gamma$ . Larger  $\text{St}$  results in larger  $T_L$  because of the sluggish response of particles to the flow. On the other hand, larger  $\gamma$  gives slightly smaller  $T_L$  because of the crossing trajectory effect (Reeks, 1977).

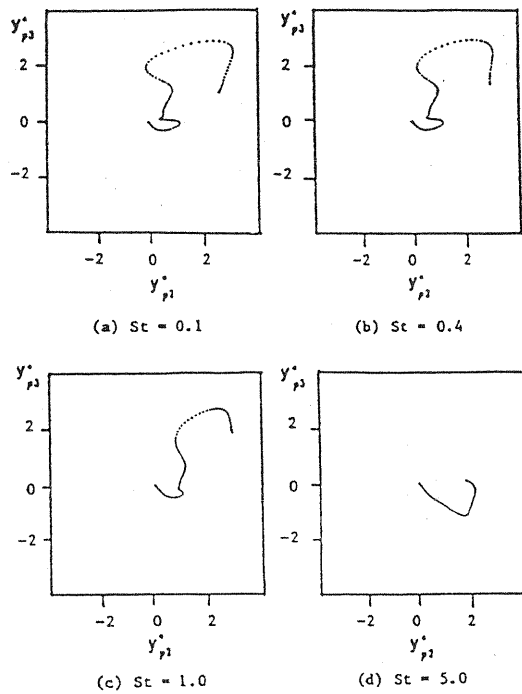


Fig. 1 Typical trajectories of a particle in a  $y-z$  plane ( $x = 0$ ) for different inertia parameters with zero fall velocity and  $k_0 u_0 T_{mE} = 0.2710$ .  $y_2^* = y_2/(u_0 T_{mE})$ ,  $y_3^* = y_3/(u_0 T_{mE})$ .

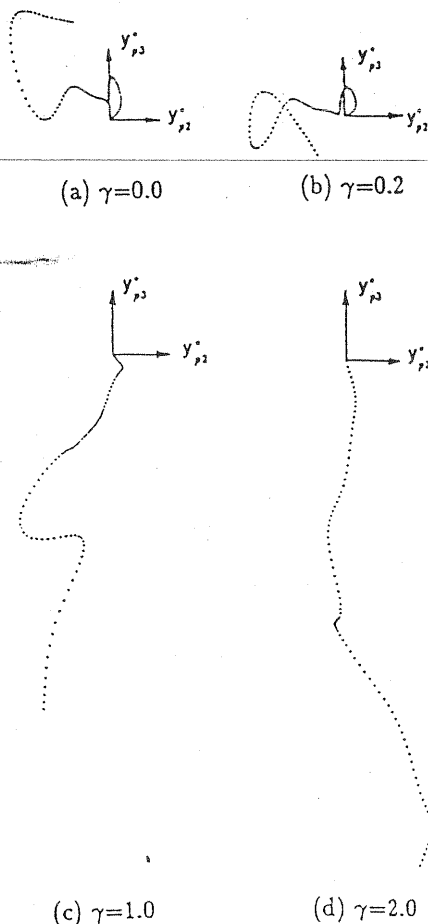


Fig. 2 Typical trajectories of a particle in a  $y-z$  plane ( $x = 0$ ) for different fall velocity  $\gamma$ , given  $St = 0.2$  and  $k_0 u_0 T_{mE} = 0.2710$ .  $y_2^* = y_2/(u_0 T_{mE})$ ,  $y_3^* = y_3/(u_0 T_{mE})$ .

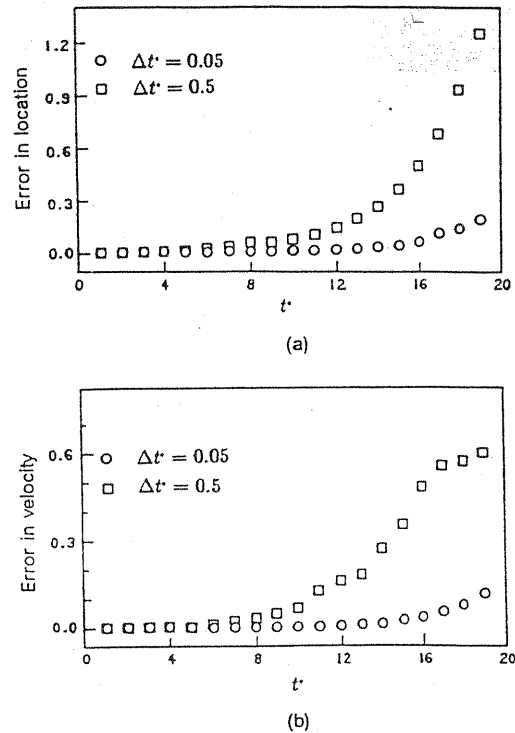


Fig. 3 Nondimensionalized global errors in the integration of equations of motion based on  $\Delta t^* = 0.01$ . Parameters are:  $St = 0.8$ ,  $k_0 u_0 T_{mE} = 0.6265$ ,  $\gamma = 1.0$ . The corresponding Lagrangian integral time of particle  $T_L^*$  is about 1.3. The number of Fourier modes  $N = 80$ . (a) Error in location; (b) error in velocity.

Table 1 Dimensionless time steps for one percent error in location at  $t^* = 4T_L^*$  ( $k_0 u_0 T_{mE} = 0.62665$ )

	$\gamma=0$	$\gamma=0.4$	$\gamma=1.0$	$\gamma=2.0$
$St=0.1$	0.2	0.2	0.1	0.1
$St=0.4$	0.1	0.1	0.08	0.06
$St=1.0$	0.08	0.06	0.05	0.04
$St=5.0$	0.05	0.04	0.03	0.02

Table 2 Dimensionless time steps for one percent error in location at  $t^* = 2$  ( $k_0 u_0 T_{mE} = 0.62665$ )

	$\gamma=0$	$\gamma=0.4$	$\gamma=1.0$	$\gamma=2.0$
$St=0.1$	0.2	0.2	0.2	0.2
$St=0.4$	0.3	0.3	0.3	0.3
$St=1.0$	0.5	0.5	0.5	0.5
$St=5.0$	1.0	1.0	0.8	0.8

size that will give an average error of one percent in the particle location after a total integration time of 2. In this case, larger time steps can be used for particles with larger inertia (larger  $St$  number), because the trajectories are less random.

Kraichnan's random Gaussian velocity field, Eq. (1), was used to provide the fluid velocity field used in the simulation. In all the simulations we used 80 Fourier modes and expected that the number of modes used in the calculations would not influence the average error in particle trajectory calculations,<sup>4</sup> because the integral scales of the velocity fields do not change when  $N$  is changed. To determine if our intuition was correct, we repeated the same simulation, but used a different number of Fourier modes in each calculation. Figure 4 shows the result of this set of calculations. Beyond 40 modes we see little change in the results when more modes are used.

The time required to accomplish a simulation for heavy

<sup>4</sup>To achieve the same uncertainty for the dispersion coefficient, the mean square displacement, or the Lagrangian velocity correlation, either a small number of Fourier modes and a large number of flow realizations or a large number of Fourier modes and smaller number of flow realizations can be used.

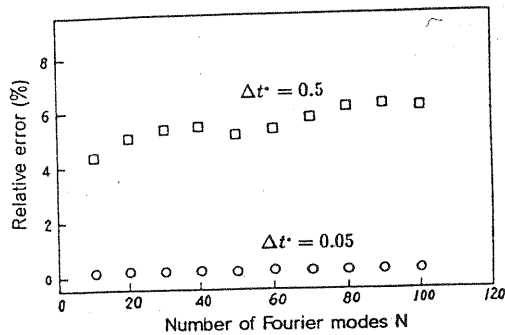


Fig. 4 The relative error in particle's location (averaged over 100 realizations of the flow) at  $f = 4T_{mE}$  (or about 5) as a function of the number of Fourier modes. Parameters are:  $St = 0.8$ ,  $\gamma = 1.0$ ,  $k_0 u_0 T_{mE} = 0.6265$ .

particle dispersion depends on the total integration time, the size of the time step, the number of Fourier modes used to simulate the fluid, and the number of particle trajectories computed. In the dispersion simulation presented in this paper, 2000 particle trajectories were calculated and 80 Fourier modes were used. The computing time on an IBM 3090 computer ranged from 2500 and 8000 seconds.

### Effect of Nonlinear Drag

When particles move with a low relative Reynolds number, the viscous drag on the particle is directly proportional to the difference in velocity between the particle and the fluid (the Stokes drag). However, when the relative Reynolds number approaches one, the drag starts to depend on the relative velocity raised to some power (the nonlinear drag). The ratio of the actual drag coefficient to the Stokes drag coefficient is called  $f$  and is given by Eq. (12). Numerical simulation is much simpler if Stokes drag can be assumed, because then each velocity component can be treated separately and the total velocity magnitude need not be computed at each time step. Before starting a simulation, one must decide if Stokes drag can be used or if the total relative velocity must be computed at each time step. One would expect that the relative velocity between the particle and the fluid would increase as the Stokes number (inertia) and  $\gamma$  (free fall velocity) increase. It would be useful to have some guidelines to help decide when nonlinear drag effects must be taken into account.

To incorporate nonlinear drag into the simulation,  $Re_p$  must be computed and updated after each time step. To calculate the  $Re_p$  we have to specify the type of particles and fluid. In our computations we assumed that the particles were glass beads ( $\rho_p = 2500 \text{ kg/m}^3$ ) and that the fluid was air with a density  $\rho = 1.22 \text{ kg/m}^3$ , kinematic viscosity  $\nu = 1.25 \times 10^{-5} \text{ m}^2/\text{s}$ . For the flow field we assumed  $u_0 = 0.2 \text{ m/s}$ ,  $T_{mE} = 0.01438 \text{ s}$ , and  $q = 9.8 \text{ m/s}^2$  for the acceleration of gravity. Then

$$Re_p = Re_0 \frac{|\mathbf{v} - \mathbf{u}|}{u_0}, \quad (18)$$

where  $Re_0 = d_p u_0 / \nu$ . For our particles and fluid this becomes

$$Re_0 = \sqrt{\frac{\rho}{\rho_p} \frac{18 u_0^3}{\nu q}} \gamma = 0.701 \gamma^{0.5}. \quad (19)$$

As the relative velocity between the particle and the fluid increases, the particle free fall velocity will be less than a similar particle falling under the influence of only Stokes drag. Figure 5 shows the mean vertical particle velocity calculated from a simulation using the nonlinear drag and a simulation using the Stokes drag. The solid lines are the analytically calculated vertical velocities of particles falling in still air. From Fig. 5 we can see that nonlinear drag effect should be considered when determining the free-fall velocity for larger  $\gamma$  (say,  $\gamma > 2$ ).

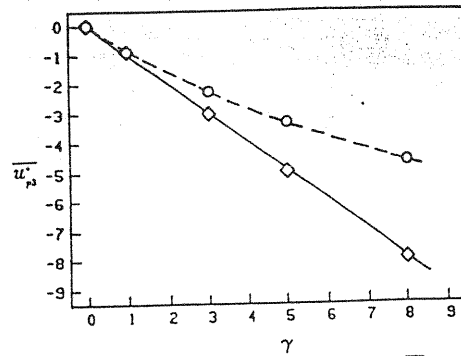


Fig. 5 Mean vertical fall velocity of a heavy particle,  $v_3^*$ , as a function of  $\gamma$  for  $St = 0.8$  and  $k_0 u_0 T_{mE} = 0.62665$ . Key: —,  $f = 1$  in still fluid (analysis);  $\circ \circ \circ$ ,  $f = 1$  in turbulent flow (simulation); - - -,  $f = 1 + 0.15 Re_p^{0.687}$  in still fluid (analysis);  $\square \square \square$ ,  $f = 1 + 0.15 Re_p^{0.687}$  in turbulent flow (simulation).

On the other hand, we found that the Stokes number had very little effect on the free-fall velocity. A very close approximation to a particle's free-fall velocity in a turbulent flow can be calculated by assuming the particle is falling through still air. Maxey (1987) found that the average settling velocity of particles in turbulent flow was larger than the free fall velocity. However, the maximum difference was about 10 percent in the extreme case of  $T_{mE} \rightarrow \infty$ . For the simulation in Fig. 5, we used  $k_0 u_0 T_{mE} = 0.62665$ , which is equivalent to a nondimensionalized  $\omega_0$  of 1.0 in Maxey's work. Maxey's Fig. 3 shows that the turbulence will increase the settling velocity by less than two percent. Thus our results as shown in Fig. 5 are in good agreement with Maxey's work.

The question of how large  $\gamma$  can be before nonlinear drag must be used in a simulation still remains. We were interested in how the simulation computed with the nonlinear drag differs from a simulation computed using Stokes drag. Therefore, we computed the ratios of the particle fluctuation velocity and diffusivity with nonlinear drag to their respective value with linear drag. We first ran some simulations at fixed  $\gamma$  and varied the Stokes number. These tests showed that the Stokes number had little effect on the computed diffusivity ratio or particle fluctuating velocity ratio for a given  $\gamma$ . The results of a computation using a Stokes number of 0.8 and a range of  $\gamma$  are shown in Figs. 6 and 7. These figures show both the fluctuation velocity ratio and the diffusivity ratio increase with increasing  $\gamma$ . From these figures we can see that nonlinear drag should be considered when  $\gamma$  is greater than two to keep the relative increase in the diffusivity due to the nonlinear drag less than 10 percent.

These findings can be explained by examining the equations of motion for the particles. If we define an effective Stokes number as  $St_e = St/f$ , and an effective drift parameter as  $\gamma_e = \gamma/f$ , the equations of motion for a particle with nonlinear drag (Eq. (13)) in terms of the effective parameters have the same form as the equations of motion for a particle under Stokes drag. Since  $f$  increases with particle free-fall velocity and is always larger than one, the effect of the nonlinear drag is to decrease the inertia and the fall velocity. Decreasing  $\gamma$  increases the dispersion coefficient and decreasing  $St$  increases the rms fluctuation velocity. Therefore, we would expect the ratios shown in Figs. 6 and 7 to increase with  $\gamma$ . Further,  $f$  is almost (not exactly) independent of the Stokes number, we thus expect  $St$  to have no influence on the ratios shown in Figs. 6 and 7.

We quantified the relative importance of the nonlinear drag in terms of  $\gamma$ , the ratio of the free fall velocity to the turbulence fluctuation velocity, rather than the particle's Reynolds number based on the fall velocity. We believe  $\gamma$  is a more proper parameter, because the relative velocity between a particle and

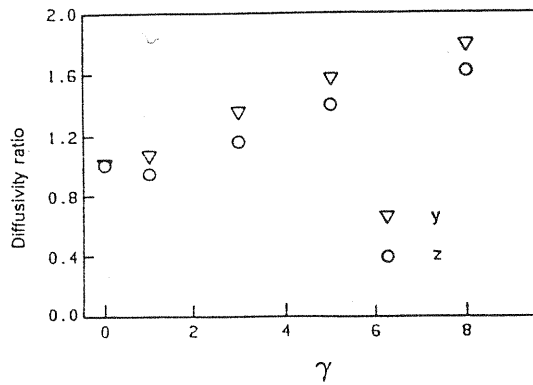


Fig. 6 The ratio of particle diffusivity with nonlinear drag to the particle diffusivity with linear drag. Parameters are:  $St = 0.8$ ,  $k_0 u_0 T_{mE} = 0.62665$ .

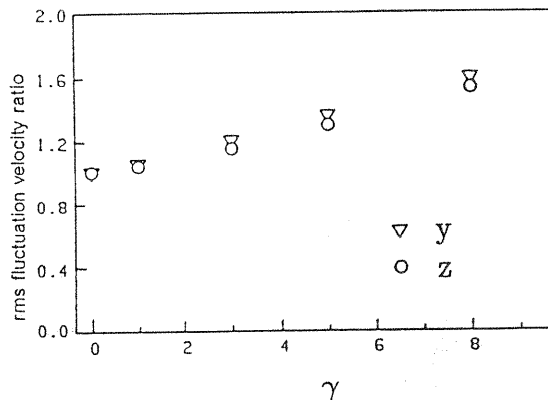


Fig. 7 The ratio of particle rms fluctuating velocity with nonlinear drag to the fluctuating velocity with linear drag. Parameters are:  $St = 0.8$ ,  $k_0 u_0 T_{mE} = 0.62665$ .  $y$  and  $z$  refer to transverse direction and vertical direction, respectively.

the flow depends on both the free-fall velocity of the particle and the fluid rms velocity,  $u_0$ .

### Comparison With Analytical Techniques

Reeks (1977) developed an approximate solution for the dispersion of particles in an isotropic, homogeneous turbulent flow using second order iteration (Phythian, 1975). The second-order iteration technique is known to give good results for dispersion of fluid particles. Reeks extended the technique to heavy particles by assuming the particle motion was governed by Stokes drag. Based on the results of the simulation presented in the last section, we would expect the approximate analysis to be valid for  $\gamma$  of two or less. In this section, we will present direct comparisons between the simulation using nonlinear drag and the analysis, which uses Stokes drag, and determine the largest  $\gamma$  that can be used with the analytical technique.

The flow field used by Reeks and the one we use in the simulation, Eq. (1), are both governed by three parameters. However, the parameters are not the same and before showing results the relationship between the parameters is needed. We used the Stokes number,  $\gamma$ , and  $m$  as the three independent parameters. Reeks used the following three parameters in his study:

$$\gamma_0 = \frac{0.62665}{m}, \quad (20)$$

$$\beta = \frac{1}{2 \cdot St \cdot m}, \quad (21)$$

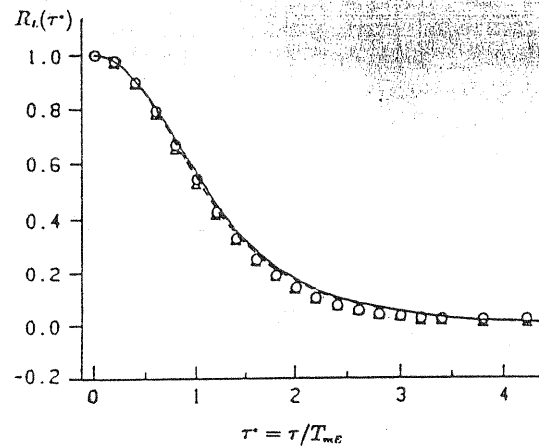


Fig. 8 Comparison of Lagrangian velocity correlations of particle for  $\gamma = 1.0$ ,  $St = 0.8$ ,  $k_0 u_0 T_{mE} = 0.62665$ . Key: ---,  $f = 1$  in transverse direction (analysis); —,  $f = 1$  in vertical direction (analysis);  $\Delta \Delta \Delta$ ,  $f = 1 + 0.15 \times Re_p^{0.687}$  in transverse direction (simulation);  $\circ \circ \circ$ ,  $f = 1 + 0.15 \times Re_p^{0.687}$  in vertical direction (simulation).

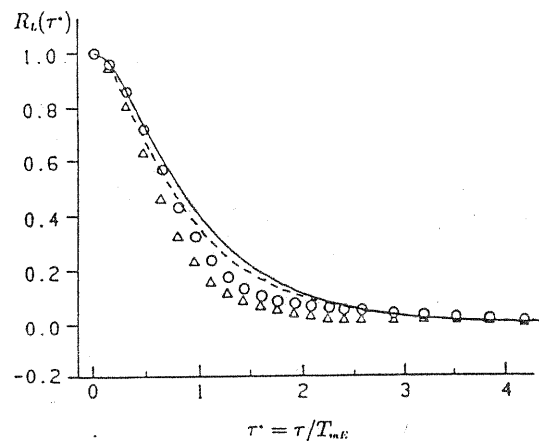


Fig. 9 Comparison of Lagrangian velocity correlations of particle for  $\gamma = 5.0$ ,  $St = 0.8$ ,  $k_0 u_0 T_{mE} = 0.62665$ . Key: ---,  $f = 1$  in transverse direction (analysis); —,  $f = 1$  in vertical direction (analysis);  $\Delta \Delta \Delta$ ,  $f = 1 + 0.15 \times Re_p^{0.687}$  in transverse direction (simulation);  $\circ \circ \circ$ ,  $f = 1 + 0.15 \times Re_p^{0.687}$  in vertical direction (simulation).

$$F_g = \frac{2 \cdot St \cdot m}{\gamma}. \quad (22)$$

To determine when the effects of nonlinear drag become significant and therefore when the analytical, second-order iteration method can no longer be used, we compared the simulation using nonlinear drag with the analysis using linear drag for a range of Stokes numbers and  $\gamma$ . All the computations were done for  $m = 0.62665$ , which is the same as used by Reeks. Figures 8 and 9 show the computed Lagrangian velocity correlations for  $\gamma$  of 1 and 5 with the Stokes number equal to 0.8 in both cases. Comparing the two plots we see that at  $\gamma = 1$  the simulation and analysis give similar results and at  $\gamma = 5$  there is considerable difference. Closer examination of the computed results show a relative decrease of 6 percent in the integral time scale  $T_L$  when the nonlinear drag is used at  $\gamma = 1$ ; while a relative decrease of 38 percent in  $T_L$  when the nonlinear drag is used at  $\gamma = 5$ . Similar calculations performed at  $\gamma = 1$  and Stokes numbers between 0.4 and 2.0 showed no additional change in the relative decrease of the integral time scale with the use of the nonlinear drag. The decrease in the integral time scale,  $T_L$ , when the nonlinear drag is used is due to the change in the effective inertia which dominates the value of  $T_L$ , as discussed earlier. We also compared the long time diffusivities determined by the simulation and the analysis and

found that the two methods agree reasonably well (within 10 percent) for  $\gamma$  of two or less and also found this result to be independent of the Stokes number.

## Conclusions

Although numerical simulation of heavy particle dispersion is very useful, performing the computations requires making decisions on the time step. With the instantaneous velocity field known, heavy particle motion can be computed by tracking the particles through the flow field by integrating the particle's equations of motion over small time steps. Since the particle's equations of motion are strongly nonlinear, one would expect the particle trajectories to be very sensitive to small numerical errors. We found that the numerical errors tended to grow exponentially, a well-known feature of a chaotic system. Although the size of the time step will depend on the integration scheme and on the number of bits being carried by the computer, we have developed some general guidelines for the effect of the particle free-fall velocity and inertia. We found that the longer the total integration time or the larger the drift parameter,  $\gamma$ , the smaller the time step that must be used to maintain the same average error in the total displacement of a particle. If the integration is over a fixed number of Lagrangian integral time scales, then the time step must be reduced as  $\gamma$  or the Stokes number increases.

We also provided some guidelines for situations where it might be necessary to include the effects of nonlinear drag when computing particle motion. For typical gas-particle flows, we found that for  $\gamma$  greater than two, nonlinear drag must be taken into account. We also found that the value of the Stokes number did not affect the relative importance of the nonlinear drag (namely, the ratios of the results based on the nonlinear

drag to their respective results based on the Stokes drag). These same results were also found when we compared the computed diffusivity from the simulation with the analytical results of a second-order iteration scheme (Reeks, 1977).

## References

- Brown, D. J., and Hutchinson, P., 1979, "The Interaction of Solid or Liquid Particles and Turbulence Fluid Flow Fields-A Numerical Simulation," *ASME JOURNAL OF FLUID ENGINEERING*, Vol. 101, pp. 265-269.
- Drummond, I. T., Duane, S., and Horgan, R. R., 1984, "Scalar Diffusion in Simulated Helical Turbulence with Molecular Diffusivity," *J. Fluid Mech.*, Vol. 138, pp. 75-91.
- Kraichnan, R. H., 1970, "Diffusion by Random Velocity Fields," *Phys. Fluids*, Vol. 13, No. 1, pp. 22-31.
- Maxey, M. R., 1987, "The Gravitational Settling of Aerosol Particles in Homogeneous Turbulence and Random Flow Fields," *J. Fluids Mech.*, Vol. 174, pp. 441-465.
- Maxey, M. R., and Riley, J. J., 1983, "The Equation of Motion for Small Rigid Particle Sphere in a Nonuniform Flow," *Phys. Fluids*, Vol. 26, pp. 883-889.
- Phythian, R., 1975, "Dispersion by Random Velocity Fields," *J. Fluid Mech.*, Vol. 67, pp. 145-153.
- Reeks, M. W., 1977, "On the Dispersion of Small Particles Suspended in an Isotropic Turbulent Field," *J. Fluid Mech.*, Vol. 83, pp. 529-546.
- Reek, M. W., 1980, "Eulerian Direct Interaction Applied to the Statistical Motion of Particles in a Turbulent Field," *J. Fluid Mech.*, Vol. 97, pp. 569-590.
- Squires, K. D., and Eaton, J. K., 1989, "Study of the Effects of Particle Loading on Homogeneous Turbulence Using Direct Numerical Simulation," *Turbulence Modification in Dispersed Multiphase Flows*, ed. E. E. Michaelides and D. E. Stock, ASME FED-Vol. 80, New York, 71 pages.
- Ueda, T., Jinno, K., Momii, K., and Machama, K., 1983, "Numerical Study of Diffusivity of Settling Particles in Homogeneous Isotropic Turbulence," *Trans. JSCE*, Vol. 15, pp. 293-296.
- Wang, L. P., and Stock, D. E., 1988, "Theoretical Method for Obtaining Lagrangian Statistics from Measurable Eulerian Statistics for Homogeneous Turbulence," *Proc. 11th Symp. on Turbulence*, Rolla, Mo, pp. B14.1-B14.12.
- Wells, M. R., and Stock, D. E., 1983, "The Effects of Crossing Trajectories on the Dispersion of Particles in a Turbulent Flow," *J. Fluid Mech.*, Vol. 136, pp. 31-62.